BENTHAM SCIENCE

CrossMark

Current Medical Imaging

Content list available at: https://benthamscience.com/journals/cmir

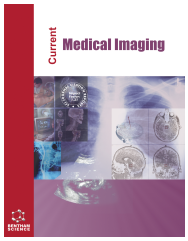

RESEARCH ARTICLE

The Diagnostic Value of a Nomogram Based on Clinical Imaging and MRI-Based Radiomic Features in Triple-Negative Breast Cancer

Liu Meng Xin[1], Ge Min[1,*], Wang Shi Wei[1,#], Lu Huan[1], Pan Zhi Yong[1] and Ding Xue Wei[1]

[1]*Department of Medical Imaging, The First Affiliated Hospital of Zhejiang Chinese Medical University, Hangzhou, China*

Abstract:

Objective:

This study aimed to determine the utility of a radiomic nomogram combined with clinical imaging and radiomic features based on MRI for the diagnosis of triple-negative breast cancer.

Methods:

Multi-parametric MRI images of 136 breast cancer patients were retrospectively analyzed, 95 cases were stratified into the training cohort, and 41 cases were selected for the test group. According to the pathological molecular typing, the patients were divided into 23 cases of triple-negative breast cancer and 113 cases of non-triple-negative breast cancer. ITK software was used to manually delineate the lesion volume region of interest (VOI), and the Pyradiomics package was used to extract radiomic features for screening and model building. The platform was then used to analyze the clinical and imaging risk factors of breast cancer to build a characteristic model separately. Finally, a radiomic nomogram was constructed by integrating the radiomic and independent clinical image features. The diagnostic performance of the model was assessed using ROC curves.

Results:

Univariate and multivariate analyses showed that the menstrual cycle, glandular density, and skin thickening were risk factors for clinical imaging characteristics of triple-negative breast cancer. The Area Under the Curve (AUC) was 0.839 and 0.826 for univariate and multivariate analysis, respectively. After screening, 11 radiomic features participated in the calculation of the radiomic score, and its AUC in the test set was 0.803. Combining it further with clinical models, the AUC improved to 0.899.

Conclusion:

The radiomic nomogram developed in this study has great value in the diagnosis of triple-negative breast cancer.

Keywords: Magnetic resonance imaging, Radiomics, Triple-negative breast cancer, AUC, Clinical models, ROC.

Article History	Received: December 26, 2022	Revised: July 16, 2023	Accepted: August 30, 2023

1. INTRODUCTION

In recent years, the morbidity and mortality of breast cancer have increased in Asia [1]. One prognostic factor of breast cancer is the intrinsic molecular subtype [2, 3]. Triple-negative breast cancer (TNBC) is a breast cancer subtype defined as lacking the expressions of estrogen receptor (ER), progesterone receptor (PR), and human epidermal receptor 2 (HER-2). It is a subtype that carries the worst prognosis because of its aggressive growth, high proliferation, and frequent metastasis [4]. Therefore, early diagnosis is very important. Magnetic resonance imaging is currently the most sensitive method for detecting breast cancer due to its versatile multimodality imaging methods. In routine imaging diagnosis, a lesion can be easily misdiagnosed as benign, thus delaying treatment. Therefore, a non-invasive, early, and accurate diagnostic method for TNBC is urgently needed. The emergence of radiomics has brought hope to solve this problem. Radiomics is a branch of medical science that aims to extract a large number of quantitative features from medical

* Address correspondence to this author at the Department of Medical Imaging, The First Affiliated Hospital of Zhejiang Chinese Medical University, Hangzhou, 310003, China; Tel: +88-182-5889-9805; E-mail: 3630163602@qq.com

#This author contributed equally to this work

images that cannot be identified with human vision alone by employing artificial intelligence algorithms. Extracted quantitative image features undergo selection with machine- and deep-learning techniques, which are subsequently used to create models that support and improve the decision-making process [5 - 8]. Radiomics uses advanced mathematical algorithms to extract and analyze texture features that cannot be recognized by the naked eye to obtain a more comprehensive picture [9]. Many studies have shown that breast cancer is a multifactorial disease, with age [10] and gland density [11] affecting the accuracy of diagnosis. The accuracy is limited for identifying TNBC in routine breast MRI. Therefore, this study combines MRI with radiomics to identify TNBC and serves to develop a nomogram from radiomic imaging features and diffusion-weighted imaging (DWI) with dynamic contrast-enhanced magnetic resonance imaging (DCE-MRI) to help diagnose triple-negative and non-triple-negative breast cancer.

2. MATERIALS AND METHODS

2.1. General Data

A total of 136 breast cancer patients who were treated in the First Affiliated Hospital of Zhejiang University of Traditional Chinese Medicine from December 2015 to May 2021 were selected. Inclusion criteria were as follows: the patients had no prior history of medical or surgical intervention, complete clinical, pathological and imaging data must be present, and patients had no other malignancies. Patients were excluded from the study if the MRI image quality was poor and if postoperative pathology was incomplete. Among them, 23 were TNBC patients, and 113 were non-TNBC patients.

2.2. Clinical Imaging Characteristics

Various clinical and imaging diagnostic indicators of patients, including age, menstrual cycle, skin thickening, nipple discharge, fibroglandular tissue (FGT), mass size, mass location, the time-intensity curve (TIC), and imaging diagnostic classification, were determined.

2.3. Instruments and Methods

All patients were scanned by a 3.0T high-field-strength superconducting Siemens MRI using a 16-channel breast-specific phased array coil. The patient was prone with the head advanced and both breasts hanging naturally within the coil. The complete scan sequence included axial T1WI, T2-stirm, DWI, and DCE sequences. DWI used a single excitation plane echo sequence. The specific parameters were: TR/TE= 8400ms/84ms, slice thickness 4.0 mm, FOV 260mm×221mm, acquisition matrix 90 × 220, and excitation time = 2, b = 800 s/mm^2. DCE-MRI used fat-suppressed axial imaging, fast low-angle excitation, and three-dimensional dynamic imaging T1WI. The specific parameters were TR/TE = 4.5ms/1.6ms, FA: 12°, slice thickness 1.0 mm, FOV 340mm × 340mm, and no spacing scan was used. The acquisition matrix was 448 × 448, excitation time = 1, single scan time = 60 s, and a mask scan was performed before contrast agent injection, which was injected intravenously at a dose of 0.2 mmol/kg at a rate of 2 mL/s. After gadopentetate meglumine injection, 5 consecutive scans were performed without interval, for a total of 6 phases.

2.4. Radiomics Analysis

Two senior radiologists used ITK-SNAP software to delineate the region of interest in DWI, DCE-3, and DCE-5 images without knowing the pathological results. The intra-class correlation coefficient (ICC) represented the consistency in diagnosis between the two physicians (ICC >0.75 was excellent agreement). The original radiomic features and the filtered features after wavelet transformation were extracted using the Pyradiomics package. Finally, a total of 851 radiomic features were extracted from one lesion. By random stratified sampling, the data sets were divided into a 7:3 training-to-validation ratio (training set n=95; validation set n=41) and a Z-score standardization was performed on the extracted features. One-way ANOVA was used for preliminary screening. The independent sample T-test (normal) or Mann-Whitney-U-test (non-normal variable) was performed for the omics features. Shapiro-Wilk-test was used for the normality test, and $p>0.05$ was considered normal. If normal was satisfied, the Levene test was used, and $p>0.05$ indicated homogeneity of variance. If the variance was homogeneous, the Student's T-test was used, and $p<0.1$ was univariate significant. If the variances were inconsistent, Welch's T-test was performed. If normality was not met, the Mann-Whitney U-test was used. Moreover, repeated variables were reduced by Spearman correlation analysis (threshold=0.6). The LASSO algorithm [12] was used, the optimal feature subset was selected, and the feature corresponding coefficient was calculated.

2.5. Pathological Analysis

All lesions were subjected to immunohistochemical detection on the specimens after surgery and classified into non-triple negative (Luminal A; Luminal B; HER-2 enriched) according to ER, PR, HER-2 and the Ki-67 classification [13] and triple-negative breast cancer.

2.6. Statistical Analysis

All statistical analyses were performed using R language version 3.6.4. The independent samples were analyzed using the Shapiro-Wilk test (normal variables) or Mann-Whitney -U-test (non-normal variables) on radiomic characteristics. Correlation analysis was performed before modeling, and an omics model was constructed using the best algorithm of the machine learning model. Then, univariate logistic regression analysis was used to find relevant clinical factors for predicting triple-negative breast cancer, and independent clinical risk factors were screened through multivariate logistic analysis to establish a clinical model. Finally, a multivariate logistic regression method was used to construct a combined model based on clinical risk factors and the radiomic scores. Afterward, a nomogram was drawn. The ROC curve of each model was used to evaluate the predictive performance of the model.

3. RESULTS

3.1. General Information and Clinical Imaging Model Construction

There were a total of 136 patients in this study, all of whom were female, including 23 TNBC patients and 113 non-TNBC patients. The univariate analysis included FGT, location, menstrual cycle, nipple discharge, palpable lump, thickened skin, and TIC. Across multivariate analysis, there was no significant difference in nipple discharge, the presence of a palpable lump, or the TIC between the two groups (Table **1**). These features were eliminated, were of clinical significance, re-incorporated into TIC, and used to construct a clinical imaging model (Fig. **1**).

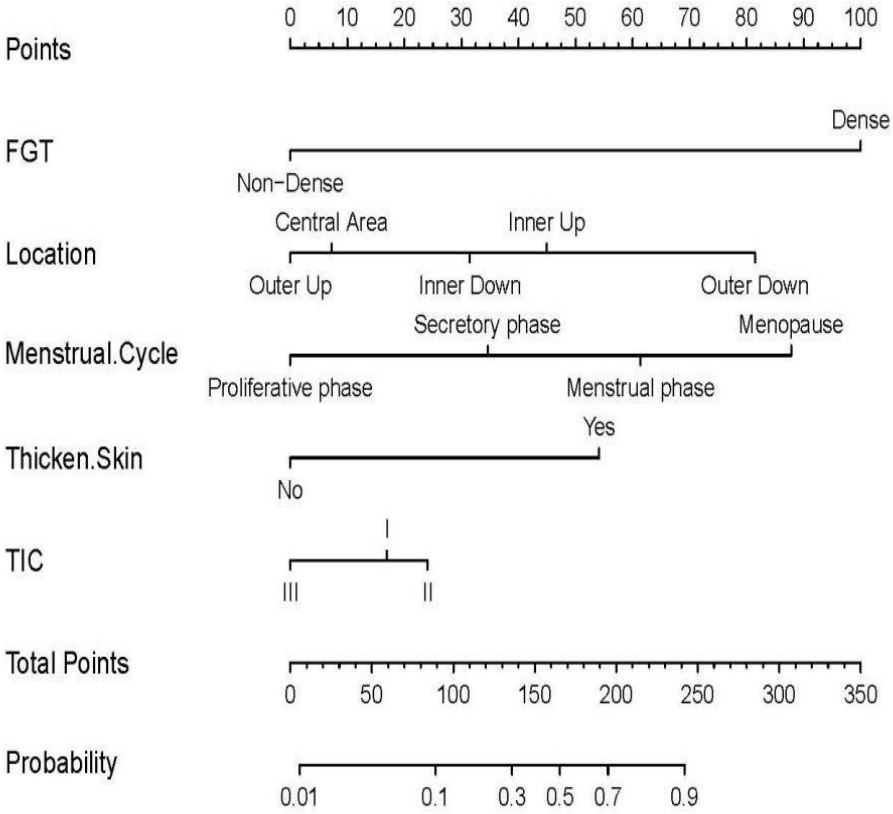

Fig. (1). Nomogram for differential diagnosis of triple-negative and non-triple-negative breast cancer by clinical imaging features.

Table 1. Clinical characteristics of patients.

Factors	Univariate Analysis			Multivariate Analysis		
	HR	95%CI	P value	HR	95%CI	P value
Age	0.997	(0.972~1.023)	0.83	-	-	-
Class (reference:3)	0.757	(0.452~1.253)	0.282	-	-	-
4	0.914	(0.212~3.716)	0.9	-	-	-
5	0.737	(0.212~3.716)	0.667	-	-	-
6	0	(0.212~3.716)	0.988	-	-	-
FGT(Non-Dense)	0.149	(0.071~0.3)	<0.001*	0.047	(0.011~0.154)	<0.001*
Location (reference: All)	-	-	-	-	-	-
Inner Down	1.048	(0.266~3.917)	0.945	1.54	(0.184~11.61)	0.676
Inner Up	2.256	(0.266~3.917)	0.096	3.765	(0.872~18.599)	0.086
Outer Down	2.933	(0.266~3.917)	0.036*	9.636	(2.192~54.67)	0.005*
Outer Up	1.086	(0.266~3.917)	0.853	0.786	(0.198~3.058)	0.727

Factors	Univariate Analysis			Multivariate Analysis		
	HR	95%CI	P value	HR	95%CI	P value
Menstrual Cycle (reference: Menopause)	-	-	-	-	-	-
Menstrual phase	0.65	(0.235~1.791)	0.401	0.357	(0.083~1.438)	0.153
Proliferative phase	0.382	(0.235~1.791)	0.041*	0.078	(0.012~0.406)	0.004*
Secretory phase	0.5	(0.235~1.791)	0.075	0.197	(0.055~0.634)	0.009*
Nipple Discharge (Yes)	2.81	(1.298~6.42)	0.011*	1.599	(0.341~7.883)	0.552
Palpable Lump (Yes)	2.308	(1.095~5.053)	0.031*	1.205	(0.251~5.465)	0.809
Thickened Skin (Yes)	3.535	(1.574~8.58)	0.003*	3.615	(0.961~14.929)	0.044*
TIC (reference:I)	-	-	-	-	-	-
II	3.5	(1.023~13.469)	0.054	0.602	(0.099~3.525)	0.572
III	3.17	(1.023~13.469)	0.037*	0.175	(0.026~1.066)	0.062

Note: *Factors that remained statistically significant ($p<0.05$).

3.2. Construction of the Radiomic Model

Two senior radiologists mapped the results in high agreement (ICC=0.90). There is no single machine learning algorithm that is optimal for any set of data. The seven most commonly used are selected according to the nature of the problem solved, the size of the dataset, the characteristics of the dataset, and whether there are labels. Seven machine learning algorithms include SVM-linear, SVM-rbf, Random-forest, Logistic, KNN, Bayes-gaussian, and Decision-tree [14 - 16]. They were used to construct the omics model, and their performances were compared. The grid search method and the ten-fold cross-validation method were used to determine the optimal parameters of each machine learning model, and the overall performance of the SVM-liner was obtained. The AUC was 0.898 and 0.803 (Figs. **2** and **3**).

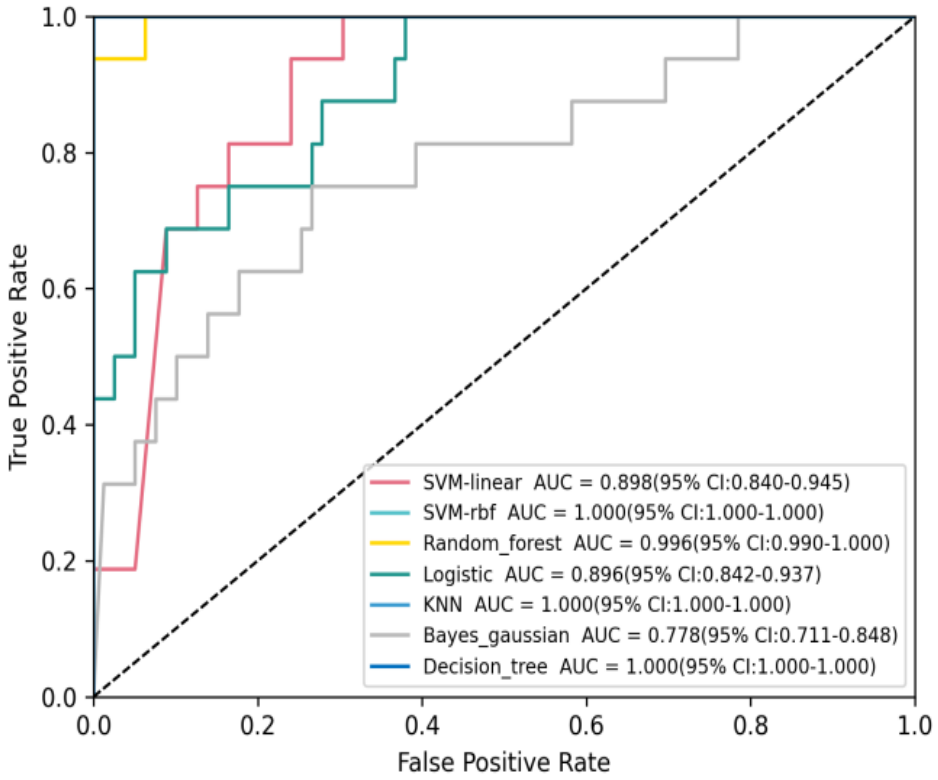

Fig. (2). ROC curve comparing the performance parameters of different machine learning models on the trained datasets.

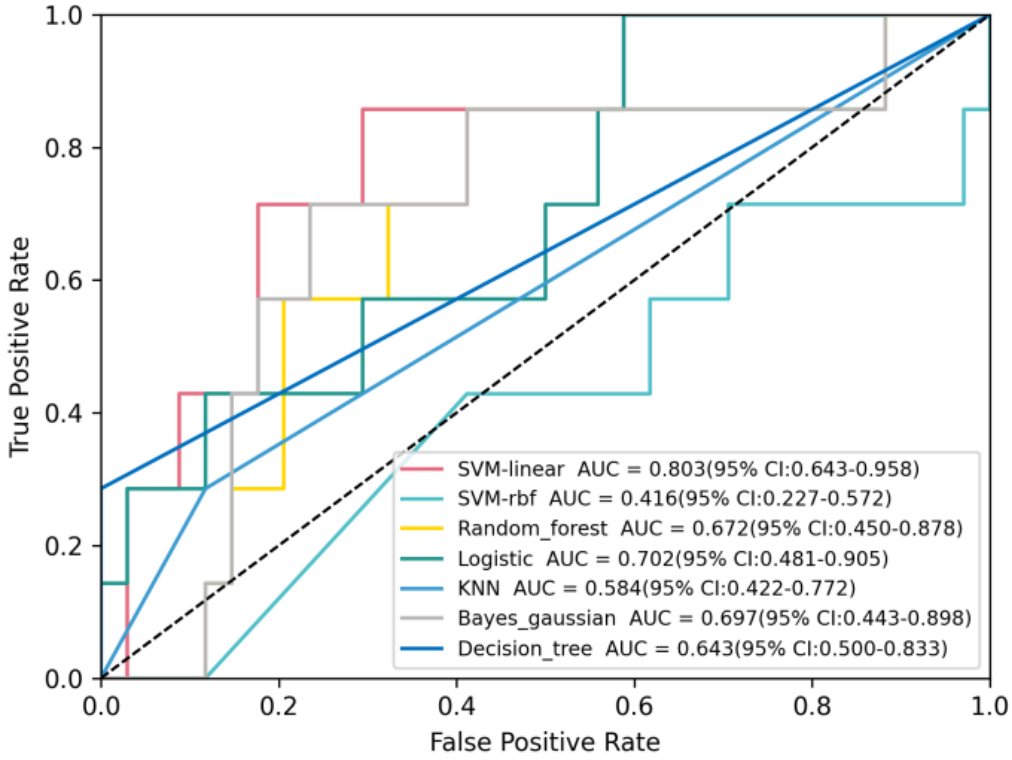

Fig. (3). ROC curve comparing the performance parameters of different machine learning models on the test datasets.

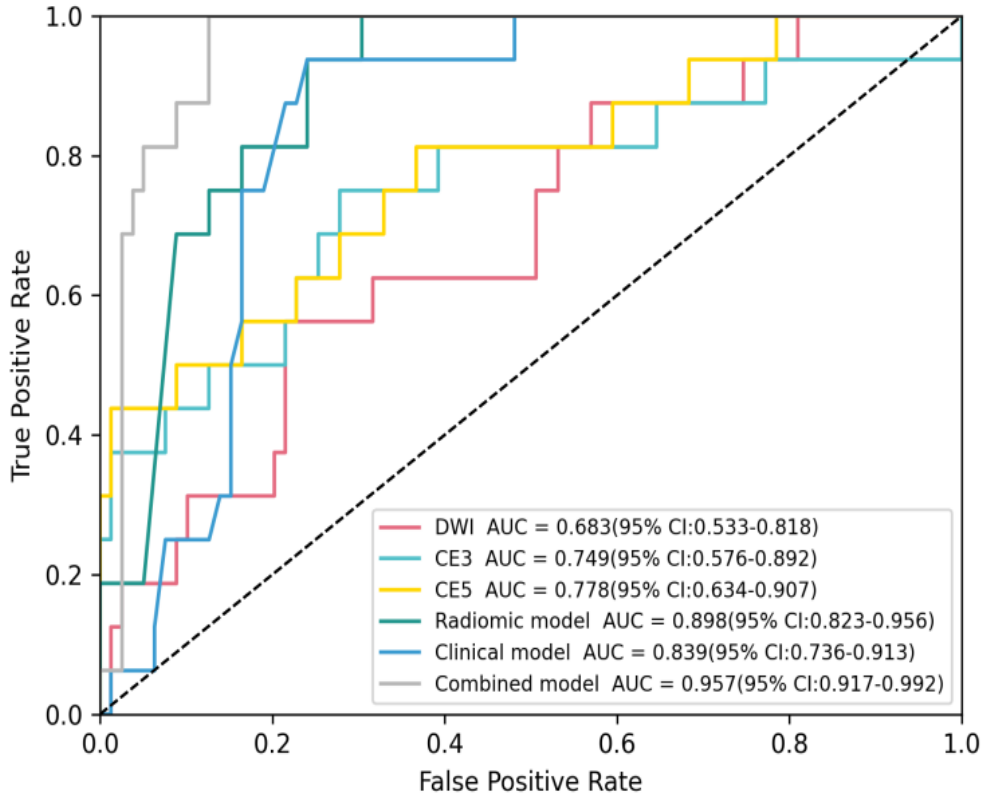

Fig. (4). ROC curves of the different models on trained datasets.

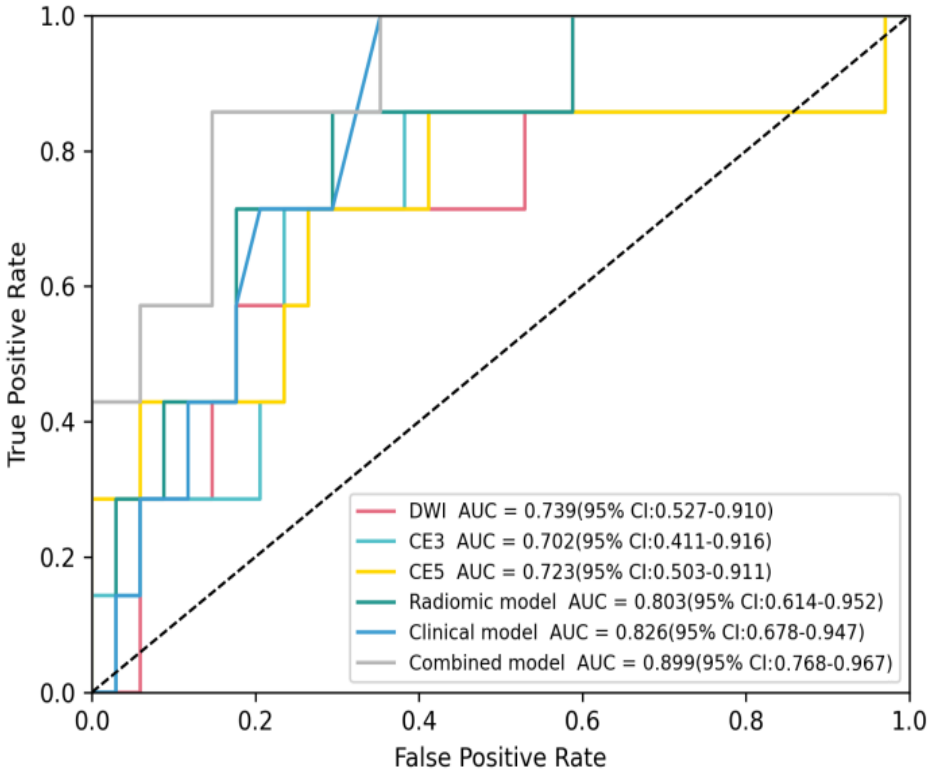

Fig. (5). ROC curves of the different models on test datasets.

3.3. Combined Model Construction and Efficacy

LASSO-logistic was used to screen the omics features from DWI, DCE-3, and DCE-5 sequences. The features of the three models were simultaneously selected, and the combined model was obtained through LASSO-logistic regression analysis. Among the features of the combined model, 5 features were derived from DWI (wavelet-HLH-glszm-Small Area Low Gray Level Emphasis, wavelet-LHL-glrlm-Short Run Low Gray Level Emphasis, wavelet-HLH-glszm-Zone Percentage, wavelet-LLL-glrlm-Long Run High Gray Level Emphasis, original-glszm-Large Area Low Gray Level Emphasis), 9 features were derived from DCE-3 (wavelet-HLH-glcm-Cluster Shade, wavelet-LHH-glrlm-Short Run Low Gray Level Emphasis, original-shape-Sphericity, wavelet-LHL-glszm-Size Zone Non Uniformity Normalized, wavelet-HLH-glrlm-Run Entropy, wavelet-LLH-glrlm-Run Length NonUniformity, wavelet-HLL-glszm-Large Area High Gray Level Emphasis, original-gldm-Small Dependence Low Gray Level Emphasis, wavelet-LHL-glszm-Zone Variance), and 11 features were derived from DCE-5 (wavelet-LHH-firstorder-Median, wavelet-HHH-glrlm-Short Run Low Gray Level Emphasis, wavelet-HLL-glcm-Cluster Shade, wavelet-HHH-glcm-Cluster Shade, original-shape-Sphericity, wavelet.LHH-glrlm-Short Run Low Gray Level Emphasis, wavelet-LLH-glrlm-Run Entropy, wavelet-HHH-firstorder-Skewness, wavelet-HLH-glszm-Large Area High Gray Level Emphasis, wavelet-HHH-firstorder-Mean, original-firstorder-Skewness). A combined model was constructed based on the radiomic features of DWI, DCE-3, and DCE-5 and the combined sequences of the three to evaluate TNBC and non-TNBC breast cancer. Features were plotted respectively. The AUC values (95% CI), sensitivity, specificity, and accuracy of each model were determined by ROC curves. According to the ROC curve, the effect of the multimodal radiomic model was better than that of a single modality (Figs. **4** and **5**), and the best predictive performance was constructed by combining clinical images and radiomic features (Fig. **6**).

4. DISCUSSION

Triple-negative breast cancer accounts for 15% to 20% of breast cancers [17]. Currently, needle biopsy is the gold standard for preoperative evaluation, and radiomics represents an emerging technology that can extract tumor tissue micro-features and analyze the micro-environment. The method can non-invasively identify TNBC and provide effective help for a clinical treatment plan. In recent years, many studies have used this method to evaluate the molecular typing of breast cancer [18], the accuracy of predicting pCR after neoadjuvant chemotherapy for TNBC [19], and its survival rate in recurrence [20]. In this study, we used clinical imaging features, DWI, DCE-3, and DCE-5 combined sequence radiomics to establish a nomogram and evaluate its diagnostic performance in TNBC.

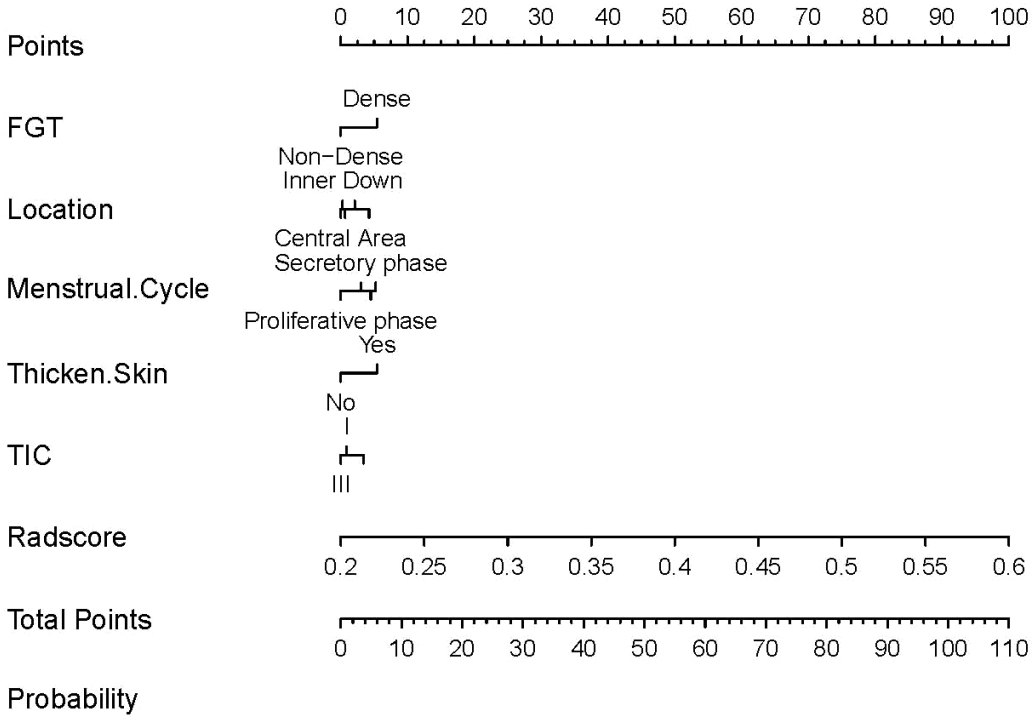

Fig. (6). Nomogram for diagnosing triple-negative breast cancer combined with clinical imaging and MRI multi-sequence features.

In this study, the age factor was excluded from the analysis of clinical imaging features because it was greatly influenced by the exclusion criteria in previous studies. The independent risk factors in this study included gland density, location, menstrual cycle and degree of skin thickening. The type of TIC curve has no statistical significance, which is consistent with previous studies [21]. Angelini *et al*. [22] found that type I curves were more common in triple-negative tumors. Considering the clinical needs, TIC types were added to the multivariate analysis.

Building predictive models and model selection are critical in radiomics to ensure reliability and stability [23 - 28]. In terms of prediction, previous research has shown that the XGBoost model outperforms other machine learning algorithms [29], and some studies have found that logistic regression is effective in the radiomic diagnostic prediction model of triple-negative type breast cancer [30, 31]. Our findings were comparable to or better than previous retrospective radiomic studies on breast MRI. We believe this is due to differences in the number of patients in the sample and the MRI radiomic characteristics used in the studies.

DWI was an effective sequence for the differential diagnosis of benign and malignant breast lesions in previous studies [32] and an effective means to predict the clinicopathological type of breast cancer [5]. Yang *et al*. [33] reported that the diagnostic performance of DWI was higher than that of TIC in DCE. In summary, this work separately and jointly modeled the DWI and DCE stage 3 and 5 sequences, of which the AUC areas of DCE-3 and 5 stages were 0.749 and 0.778, respectively.

There were some discrepancies in the analysis of the radiomic results for the diagnosis of breast cancer by multiparametric MRI. The AUC of the radiomic features based on the pharmacokinetic parameter map of DCE-MRI was 0.836, which may be related to the inclusion of malignant lesions in this study. Many studies have focused on the radiological analysis of DCE-MRI [34, 35]. For example, the imaging features of DCE-MRI can predict Luminal type A and Luminal type B [36] and distinguish between histological and immunohistochemical breast cancer subtypes [37]. Due to no uniform standard for selecting sequences in breast cancer MRI radiomics studies, imaging of features (which are highly related to the sequence type utilized) is rarely used to distinguish TNBC from non-TNBC. Many studies have shown that the diagnostic performance of the multi-sequence model is better than that of the single-sequence model. Zhang *et al*. [34] included multiple sequences of T1WI, T2WI, ADC, DKI, and DCE-MRI for comparison. The results showed that the fusion model of T2WI, DKI, and DCE-MRI has high diagnostic performance (AUC=0.921). A separate study [38] that combined 6 phases of DCE-MRI and 3 b-value images of DWI for machine learning showed that SVM has the highest accuracy in comparing TNBC and non-TNBC. The rate was as high as 91.0%. In this study, the combination of three sequences yielded an AUC area of 0.898. Few studies have added clinical features to the prediction model. Therefore, our study predicted TNBC by combining clinical imaging features and dynamic imaging features using DWI and DCE. The

results showed high diagnostic performance with an overall accuracy of 89.5%. In conclusion, the multi-parameter, multi-sequence joint model can better demonstrate the characteristics of TNBC.

A meta-analysis showed that MRI-based radiomics has good diagnostic value for TNBC with high specificity and a high AUC, which increases confidence in TNBC prediction [39]. However, MRI-based radiomics uses artificial intelligence algorithms to extract a large number of radiomics features from MRI images by employing artificial intelligence algorithms. Extracted radiomics image features undergo selection with machine and deep-learning techniques and are subsequently used to create models that allow clinicians to infer the molecular status of a tumour in a non-invasive manner, enabling assessment of tumour heterogeneity both temporally and spatially [40, 41]. Several studies [35, 42, 43] have applied radiomics based on breast MRI to distinguish TNBC from other subtypes. The sensitivity and specificity reported in these studies are different. The results of this study are slightly different from those of previous studies. The main explanation for these differences is probably that the methodology varied considerably among studies, particularly in MRI sequence selection, segmentation of breast tumours, feature extraction and selection, model construction, and validation. The high specificity and AUC will greatly improve the communication between doctors and patients, facilitate clinical decision-making, enable the development of optimal treatment plans, and improve clinical outcomes.

This study has certain limitations. First, the sample size of this study is limited, and many cases need to be externally verified for the development of nomograms. Secondly, the clinical factors included in this study were limited; biochemical and pathological types should be further analyzed. Thirdly, manual delineation of ROI is prone to subjective bias.

CONCLUSION

In conclusion, the nomogram based on clinical imaging risk factors and breast DCE-MRI radiomic features can better differentiate TNBC from non-TNBC compared to single modality methods. This combined system can provide a non-invasive method for clinical preoperative TNBC characterization.

AUTHORS' CONTRIBUTIONS

Liu Mengxin and Ge Min wrote the main manuscript text, and Wang Shiwei, Lu Huan, Pan Zhiyong, and Ding Xuewei prepared figures and data processing. All authors reviewed the manuscript.

LIST OF ABBREVIATIONS

VOI	=	Volume Region of Interest
AUC	=	Area Under Curve
TNBC	=	Triple-Negative Breast Cancer
ER	=	Estrogen Receptor

ETHICS APPROVAL AND CONSENT TO PARTICIPATE

The Ethics Committee of the First Affiliated Hospital of Zhe-jiang Chinese Medical University has approved this study (ethics approval date: 2021-06-17 number:2021-KL-073-01).

HUMAN AND ANIMAL RIGHTS

No animals were used in this research. All procedures performed in studies involving human participants were in accordance with the ethical standards of institutional and/or research committee and with the 1975 Declaration of Helsinki, as revised in 2013.

CONSENT FOR PUBLICATION

Informed consent was obtained from all participants.

STANDARDS OF REPORTING

STROBE guidelines were followed.

AVAILABILITY OF DATA AND MATERIALS

The datasets used or analyzed during the current study are available from the corresponding author [G.M] upon reasonable request.

FUNDING

This study was supported by the Zhejiang Provincial Natural Science Foundation of China (LGF21H180003) and the Zhejiang Traditional Chinese Medicine Science and Technology Project (2022ZB132). The funders had roles in the design of the study, data collection, analysis, and manuscript writing.

CONFLICT OF INTEREST

The authors declare that they have no competing interests.

ACKNOWLEDGEMENTS

The authors would like to express sincere gratitude to their team and all their friends and family members.

REFERENCES

[1] Kim Y, Yoo KY, Goodman MT. Differences in incidence, mortality and survival of breast cancer by regions and countries in Asia and contributing factors. Asian Pac J Cancer Prev 2015; 16(7): 2857-70. [http://dx.doi.org/10.7314/APJCP.2015.16.7.2857] [PMID: 25854374]

[2] Nguyen PL, Taghian AG, Katz MS, *et al.* Breast cancer subtype approximated by estrogen receptor, progesterone receptor, and HER-2 is associated with local and distant recurrence after breast-conserving therapy. J Clin Oncol 2008; 26(14): 2373-8. [http://dx.doi.org/10.1200/JCO.2007.14.4287] [PMID: 18413639]

[3] Johansson ALV, Trewin CB, Hjerkind KV, Ellingjord-Dale M, Johannesen TB, Ursin G. Breast cancer-specific survival by clinical subtype after 7 years follow-up of young and elderly women in a nationwide cohort. Int J Cancer 2019; 144(6): 1251-61. [http://dx.doi.org/10.1002/ijc.31950] [PMID: 30367449]

[4] Vagia E, Mahalingam D, Cristofanilli M. The landscape of targeted therapies in TNBC. Cancers 2020; 12(4): 916. [http://dx.doi.org/10.3390/cancers12040916] [PMID: 32276534]

[5] Ni M, Zhou X, Liu J, *et al.* Prediction of the clinicopathological subtypes of breast cancer using a fisher discriminant analysis model based on radiomic features of diffusion-weighted MRI. BMC Cancer 2020; 20(1): 1073. [http://dx.doi.org/10.1186/s12885-020-07557-y] [PMID: 33167903]

[6] Li Q, Dormer JD, Daryani P, Chen D, Zhang Z, Fei B. Radiomics analysis of MRI for predicting molecular subtypes of breast cancer in young women. Proc SPIE 2019; 10950: 148. [http://dx.doi.org/10.1117/12.2512056] [PMID: 32528211]

[7] Fan M, Li H, Wang S, Zheng B, Zhang J, Li L. Radiomic analysis reveals DCE-MRI features for prediction of molecular subtypes of breast cancer. PLoS One 2017; 12(2): e0171683. [http://dx.doi.org/10.1371/journal.pone.0171683] [PMID: 28166261]

[8] Leithner D, Horvat JV, Marino MA, *et al.* Radiomic signatures with contrast-enhanced magnetic resonance imaging for the assessment of breast cancer receptor status and molecular subtypes: Initial results. Breast Cancer Res 2019; 21(1): 106. [http://dx.doi.org/10.1186/s13058-019-1187-z] [PMID: 31514736]

[9] Lambin P, Rios-Velazquez E, Leijenaar R, *et al.* Radiomics: Extracting more information from medical images using advanced feature analysis. Eur J Cancer 2012; 48(4): 441-6. [http://dx.doi.org/10.1016/j.ejca.2011.11.036] [PMID: 22257792]

[10] Iyengar NM, Morris PG, Zhou XK, *et al.* Menopause is a determinant of breast adipose inflammation. Cancer Prev Res 2015; 8(5): 349-58. [http://dx.doi.org/10.1158/1940-6207.CAPR-14-0243] [PMID: 25720743]

[11] Mann RM, Athanasiou A, Baltzer PAT, *et al.* Breast cancer screening in women with extremely dense breasts recommendations of the European Society of Breast Imaging (EUSOBI). Eur Radiol 2022; 32(6): 4036-45. [http://dx.doi.org/10.1007/s00330-022-08617-6] [PMID: 35258677]

[12] McNeish DM. Using lasso for predictor selection and to assuage overfitting: A method long overlooked in behavioral sciences. Multivariate Behav Res 2015; 50(5): 471-84. [http://dx.doi.org/10.1080/00273171.2015.1036965] [PMID: 26610247]

[13] Goldhirsch A, Winer EP, Coates AS, *et al.* Personalizing the treatment of women with early breast cancer: Highlights of the ST gallen international expert consensus on the primary therapy of early breast cancer 2013. Ann Oncol 2013; 24(9): 2206-23. [http://dx.doi.org/10.1093/annonc/mdt303] [PMID: 23917950]

[14] Han Y, Ma Y, Wu Z, *et al.* Histologic subtype classification of non-small cell lung cancer using PET/CT images. Eur J Nucl Med Mol Imaging 2021; 48(2): 350-60. [http://dx.doi.org/10.1007/s00259-020-04771-5] [PMID: 32776232]

[15] Dalal V, Carmicheal J, Dhaliwal A, Jain M, Kaur S, Batra SK. Radiomics in stratification of pancreatic cystic lesions: Machine learning in action. Cancer Lett 2020; 469: 228-37. [http://dx.doi.org/10.1016/j.canlet.2019.10.023] [PMID: 31629933]

[16] Fontaine P, Riet FG, Castelli J, *et al.* Comparison of feature selection in radiomics for the prediction of overall survival after radiotherapy for hepatocellular carcinoma. Annu Int Conf IEEE Eng Med Biol Soc 2020; 2020: 1667-70. [http://dx.doi.org/10.1109/EMBC44109.2020.9176724] [PMID: 33018316]

[17] Yin L, Duan JJ, Bian XW, Yu S. Triple-negative breast cancer molecular subtyping and treatment progress. Breast Cancer Res 2020; 22(1): 61. [http://dx.doi.org/10.1186/s13058-020-01296-5] [PMID: 32517735]

[18] Davey MG, Davey MS, Boland MR, Ryan ÉJ, Lowery AJ, Kerin MJ. Radiomic differentiation of breast cancer molecular subtypes using pre-operative breast imaging - A systematic review and meta-analysis. Eur J Radiol 2021; 144: 109996. [http://dx.doi.org/10.1016/j.ejrad.2021.109996] [PMID: 34624649]

[19] Jimenez JE, Abdelhafez A, Mittendorf EA, *et al.* A model combining pretreatment MRI radiomic features and tumor-infiltrating lymphocytes to predict response to neoadjuvant systemic therapy in triple-negative breast cancer. Eur J Radiol 2022; 149: 110220. [http://dx.doi.org/10.1016/j.ejrad.2022.110220] [PMID: 35193025]

[20] Kamiya S, Satake H, Hayashi Y, *et al.* Features from MRI texture analysis associated with survival outcomes in triple-negative breast cancer patients. Breast Cancer 2022; 29(1): 164-73. [http://dx.doi.org/10.1007/s12282-021-01294-1] [PMID: 34529241]

[21] Angelini G, Marini C, Iacconi C, *et al.* Magnetic resonance (MR) features in triple negative breast cancer (TNBC) *vs* receptor positive cancer (nTNBC). Clin Imaging 2018; 49: 12-6. [http://dx.doi.org/10.1016/j.clinimag.2017.10.016] [PMID: 29120811]

[22] Uematsu T, Kasami M, Yuen S. Triple-negative breast cancer: Correlation between MR imaging and pathologic findings. Radiology 2009; 250(3): 638-47. [http://dx.doi.org/10.1148/radiol.2503081054] [PMID: 19244039]

[23] Papanikolaou N, Matos C, Koh DM. How to develop a meaningful radiomic signature for clinical use in oncologic patients. Cancer Imaging 2020; 20(1): 33. [http://dx.doi.org/10.1186/s40644-020-00311-4] [PMID: 32357923]

[24] Choy G, Khalilzadeh O, Michalski M, *et al.* Current applications and future impact of machine learning in radiology. Radiology 2018; 288(2): 318-28. [http://dx.doi.org/10.1148/radiol.2018171820] [PMID: 29944078]

[25] Park EK, Lee K, Seo BK, *et al.* Machine learning approaches to radiogenomics of breast cancer using low-dose perfusion computed tomography: Predicting prognostic biomarkers and molecular subtypes. Sci Rep 2019; 9(1): 17847. [http://dx.doi.org/10.1038/s41598-019-54371-z] [PMID: 31780739]

[26] Eun NL, Kang D, Son EJ, *et al.* Texture analysis with 3.0-T MRI for association of response to neoadjuvant chemotherapy in breast cancer. Radiology 2020; 294(1): 31-41. [http://dx.doi.org/10.1148/radiol.2019182718] [PMID: 31769740]

[27] Parmar C, Grossmann P, Bussink J, Lambin P, Aerts HJWL. Machine learning methods for quantitative radiomic biomarkers. Sci Rep 2015; 5(1): 13087. [http://dx.doi.org/10.1038/srep13087] [PMID: 26278466]

[28] Zhang B, He X, Ouyang F, *et al.* Radiomic machine-learning classifiers for prognostic biomarkers of advanced nasopharyngeal carcinoma. Cancer Lett 2017; 403: 21-7. [http://dx.doi.org/10.1016/j.canlet.2017.06.004] [PMID: 28610955]

[29] Chen T, Guestrin C. XGBoost: A scalable tree boosting system. The 22nd ACM SIGKDD International Conference. New York. 2016; pp. 785-94.

[30] Monti S, Aiello M, Incoronato M, *et al.* DCE-MRI pharmacokinetic-based phenotyping of invasive ductal carcinoma:A radiomic study for prediction of histological outcomes. Contrast Media Mol Imaging 2018; 2018: 1-11. [http://dx.doi.org/10.1155/2018/5076269] [PMID: 29581709]

[31] Perou CM, Sørlie T, Eisen MB, *et al.* Molecular portraits of human breast tumours. Nature 2000; 406(6797): 747-52. [http://dx.doi.org/10.1038/35021093] [PMID: 10963602]

[32] Amornsiripanitch N, Bickelhaupt S, Shin HJ, *et al.* Diffusion-weighted MRI for unenhanced breast cancer screening. Radiology 2019; 293(3): 504-20. [http://dx.doi.org/10.1148/radiol.2019182789] [PMID: 31592734]

[33] Yang X, Dong M, Li S, *et al.* Diffusion-weighted imaging or dynamic contrast-enhanced curve: A retrospective analysis of contrast-enhanced magnetic resonance imaging–based differential diagnoses of benign and malignant breast lesions. Eur Radiol 2020; 30(9): 4795-805. [http://dx.doi.org/10.1007/s00330-020-06883-w] [PMID: 32350660]

[34] Zhang Q, Peng Y, Liu W, *et al.* Radiomics based on multimodal MRI for the differential diagnosis of benign and malignant breast lesions. J Magn Reson Imaging 2020; 52(2): 596-607. [http://dx.doi.org/10.1002/jmri.27098] [PMID: 32061014]

[35] Ma M, Gan L, Jiang Y, *et al.* Radiomics analysis based on automatic image segmentation of DCE-MRI for predicting triple-negative and nontriple-negative breast cancer. Comput Math Methods Med 2021; 2021: 1-7. [http://dx.doi.org/10.1155/2021/2140465] [PMID: 34422088]

[36] Grimm LJ, Zhang J, Mazurowski MA. Computational approach to radiogenomics of breast cancer: Luminal A and luminal B molecular subtypes are associated with imaging features on routine breast MRI extracted using computer vision algorithms. J Magn Reson Imaging 2015; 42(4): 902-7. [http://dx.doi.org/10.1002/jmri.24879] [PMID: 25777181]

[37] Waugh SA, Purdie CA, Jordan LB, *et al.* Magnetic resonance imaging texture analysis classification of primary breast cancer. Eur Radiol 2016; 26(2): 322-30. [http://dx.doi.org/10.1007/s00330-015-3845-6] [PMID: 26065395]

[38] Xie T, Wang Z, Zhao Q, *et al.* Machine learning-based analysis of MR multiparametric radiomics for the subtype classification of breast cancer. Front Oncol 2019; 9: 505. [http://dx.doi.org/10.3389/fonc.2019.00505] [PMID: 31259153]

[39] Sha YS, Chen JF. MRI-based radiomics for the diagnosis of triple-negative breast cancer: A meta-analysis. Clin Radiol 2022; 77(9): 655-63. [http://dx.doi.org/10.1016/j.crad.2022.04.015] [PMID: 35641339]

[40] Leithner D, Mayerhoefer ME, Martinez DF, *et al.* Non-invasive assessment of breast cancer molecular subtypes with multi-parametric magnetic resonance imaging radiomics. J Clin Med 2020; 9(6): 1853. [http://dx.doi.org/10.3390/jcm9061853] [PMID: 32545851]

[41] Leithner D, Bernard-Davila B, Martinez DF, *et al.* Radiomic signatures derived from diffusion-weighted imaging for the assessment

of breast cancer receptor status and molecular subtypes. Mol Imaging Biol 2020; 22(2): 453-61.
[http://dx.doi.org/10.1007/s11307-019-01383-w] [PMID: 31209778]

[42] Wang Q, Mao N, Liu M, *et al.* Radiomic analysis on magnetic resonance diffusion weighted image in distinguishing triple-negative breast cancer from other subtypes: A feasibility study. Clin Imaging 2021; 72: 136-41.
[http://dx.doi.org/10.1016/j.clinimag.2020.11.024] [PMID: 33242692]

[43] Wu J, Sun X, Wang J, *et al.* Identifying relations between imaging phenotypes and molecular subtypes of breast cancer: Model discovery and external validation. J Magn Reson Imaging 2017; 46(4): 1017-27.
[http://dx.doi.org/10.1002/jmri.25661] [PMID: 28177554]